

# Multi-objective Sliding Mode Control of a Wind Farm with Permanent Magnet Synchronous Generator

Ali Bagheri  
[ali.bagheria54@gmail.com](mailto:ali.bagheria54@gmail.com)  
Isfahan Science and Research Branch,  
Islamic Azad University, Isfahan, Iran

Shahrokh Shojaeian  
[Shojaeian@iaukhsh.ac.ir](mailto:Shojaeian@iaukhsh.ac.ir)  
Khomeinshahr Branch, Islamic Azad  
University, Isfahan, Iran

Javad Pourabadeh  
[Pourabadeh@iaukhsh.ac.ir](mailto:Pourabadeh@iaukhsh.ac.ir)  
Khomeinshahr Branch, Islamic Azad  
University, Isfahan, Iran

**Abstract**— In this paper, the sliding mode control method has been used to optimize the performance of a wind Farm with the permanent magnet synchronous generator connected to the utility grid through two back-to-back PWM converters. The first goal for the control system is maximum power point tracking. On the other generated power is injected by using to the grid, by applying the sliding mode control to them at wind speed variations, one can regulate the DC link voltage as well as the power factor from the grid point of view. The later is needed to be unit or close to it. In order to actualize this purpose, appropriate sliding surfaces are defined to extract the required control law, and insure stability in Lyapunov's method.

**Keywords**— Maximum Power Point Tracking, Magnet Synchronous Generator, Robustness, Sliding Mode

## I. INTRODUCTION

Application of renewable energies is one of the most important strategies of countries in the recent decays. Nowadays, as the contribution of renewable energy sources in the supply of the electric loads increases, the structure and behaviour of these energy sources should be carefully investigated. In the meantime, wind is known as the most effective and highly consumed type of renewable energy. On the other hand, as the wind Farms capacity increases, it will be expected that they can, play an effective role in the network frequency and voltage control. In this paper, study of a wind Farm containing the permanent magnet synchronous generator is under consideration.

The angular stability of power systems, including large wind farms, has been studied in [1] and shows that the variable speed wind turbine reactive power control mode will directly influence the synchronous generators angular stability.

References [2, 3] have dealt with the reactive power controllability in wind turbines based on doubly-fed induction generators. Meanwhile, they have considered the limitations of converters and generators in their simulations. A doubly-fed induction generator (DFIG)

performance after the occurrence of voltage sag is one of the most important discussions dealt with in such generators. Reference [4, 5] try to optimize this index in different methods.

Reference [6] studies the effect of voltage sag on the doubly-fed induction generator performance and proposes effective methods for the generator control in any state.

Extraction of maximum possible power from wind energy at different wind speeds has always been a basic issue in wind turbines utilization. In [7], the variable speed wind turbine operating point is regulated by the fuzzy method under maximum power conditions. This applies while turbine performance at the optimized point has been actualized in [8, 9] via intelligent algorithms based on the neural network, and in [10, 11] through the DC link voltage control. While tracking the optimized point at wind different speeds, the tip linear speed limitation has also been considered in [12]. In [13], a method has been proposed in which a variable frequency transformer will decrease the wind power station output power fluctuations, whereas in [14], the pitch angle control is used to render wind turbine output fluctuations less effective in the fuzzy method. In [15], it has been recommended to smoothen the PMSG-based wind turbine output power using the pitch angle coordinated control and power electronic converter. In [15], output power low frequency fluctuations will be compensated by the pitch angle control, and high frequency fluctuations by the DC link voltage control. [16] shows that as wind power stations based on doubly-fed induction generators are replaced and their production power increases in the power grid, frequency control will face serious challenges. In this connection, [17,18] compare the mode of response of traditional and variable speed wind turbine power stations to frequency loss and refer to the existing methods of wind turbines contribution in frequency control.

[19] shows that since the equivalent constant of inertia in wind generator is a significant value compared with that in traditional generator, by controlling wind turbines, the



system frequency can be optimized even better than when wind energy has no contribution in the power system. In [20], by regulating the rotor flux vector magnitude and angle, effort has been made to control wind turbines electric torque in early moments after turbulence.

In [21], beside adding a control loop for wind turbines contribution in the short term frequency control, a slow PI controller has also been used so that upon the frequency instantaneous behaviour optimization, the rotor speed will smoothly return to the reference value. Otherwise, the rotor speed quick return to the reference value causes another turbulence to be observed in the system frequency curve.

Maximum power point tracking (MPPT) control systems cause power capture, power quality and can be used to control aerodynamic chattering and mechanical stresses. Furthermore, by developing power electronics technology, it will be possible to use high performance converters in order to get maximum power from the generators. For this reason, the variable speed wind turbine generator system very well suits the wind Farms.

Recently, application of the permanent magnet synchronous generator (PMSG) is growing for different reasons including the very high torque value which can be obtained by the generator at low speeds, for the generator is directly connected to the turbine with no gearbox and make less chattering during operation, there will be negligible loss in the rotor, with no need for any external excitation current. As a result, the efficiency of PMSG- based wind Farms can be higher than that of other generators and render it a perfectly logical choice. In PMSG-based wind generators, application of power electronic advanced technology has led, beside equipment expense decrease, to the fact that with the help of controlled converters, a large amount and controllable power can be injected to the grid. For speed regulation and coping with the effect of wind speed fluctuations on the generator output power, a speed regulation system is required, by which a wind turbine will be able, at wind speed variations, to operate at a speed as close as possible to its optimized speed. This implies the necessity of maximum power point tracking. In our recommended method, two types of controller, the pitch angle controller and the power controller, have been used to regulate the output power. In this paper, the pitch angle controller and the grid connected to the PMSG-based variable speed wind generator have been studied to increase the power generated with unit power factor. The typical system configuration includes a wind turbine generator, a PMSG, a PWM rectifier on the generator side and a PWM converter on the grid side connected to each other by the capacitor DC link. The system block diagram has been shown in Fig.1. The combination of the MPPT strategy technique with the sliding mode control (SMC) method thus presents a properly acceptable performance

under system uncertainties. For the pitch angle control, regarding wind speed variability, the sliding mode method has been applied to both converters.

## II. THE SYSTEM MODELLING

### A. Wind turbine model

The speed controller aims to extract wind maximum energy at powers lower than the rated value, while the grid side converter aims at energy transfer from the PMSG to the utility grid by regulating the DC link voltage, obtaining unit power factor and decreasing current distortion.

A wind turbine is not by itself able to perfectly capture maximum wind energy. A wind turbine power production is given by [22]:

$$P_{turbine} = \frac{1}{2} \rho A C_p (\lambda, \beta) V^3 \quad (1)$$

where  $\rho$  is the air density ( $1.225 \text{ kg/m}^3$ ),  $A$  is the area swept by the blade,  $C_p(\text{m}^2)$  is the energy conversion coefficient and  $\lambda$  is the tip speed ratio which is in relation with the linear speed ratio and turbine axis speed  $\omega_m$  [23]:

$$\lambda = \frac{\omega_m R}{V} \quad (2)$$

$V$  is the wind linear speed in m/s and  $R$  is the rotor radius in meters. The turbine mechanical torque can be written as follows:

$$T_m = \frac{1}{2} \rho A C_p (\lambda, \beta) V^3 \frac{1}{\omega_m} \quad (3)$$

The  $C_p$  function is usually shown by the following equation [23]:

$$C_p = \frac{1}{2} \left( \frac{116}{\lambda_i} - 0.4\beta - 5 \right) e^{-\left(\frac{21}{\lambda_i}\right)} \quad (4)$$

Where  $\lambda_i$  is itself a function of  $\lambda$  and  $\beta$ :

$$\frac{1}{\lambda_i} = \frac{1}{\lambda + 0.08\beta} - \frac{0.035}{\beta^3 + 1} \quad (5)$$

Where  $\beta$  is the pitch angle.  $C_p$  and correspondingly the turbine production power achieve their highest value at a certain  $\lambda$  ( $\lambda_{opt}$ ). For example, with  $\beta=0$ :  $\lambda_{opt}=2.1$  and  $C_{pmax}=0.41$ , Consequently.

$$P_{turbine} = \frac{1}{2} \rho A C_{pmax} V^3 \quad (6)$$

The behavior of  $C_p(\lambda, \beta)$  for the different pitch angle values has been mentioned in [11]. At any particular wind speed, there exists a specific point in the wind generator power characteristic where the output power is maximized. So, it is necessary to keep the rotor speed at this optimum value of the tip speed ratio,  $\lambda_{opt}$ . Then the system can operate at the peak of the  $P(\omega)$  curve when wind speed changes and the maximum power is continuously extracted from the

wind as shown in Fig.2. Thus, by connecting the curves maximum(peak) points, the maximum output for wind speed will be obtained and followed for maximum power operation.

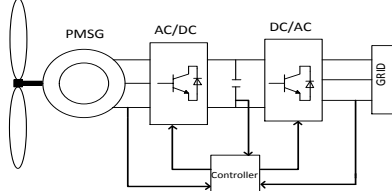


Fig.1. Block diagram of WECS.

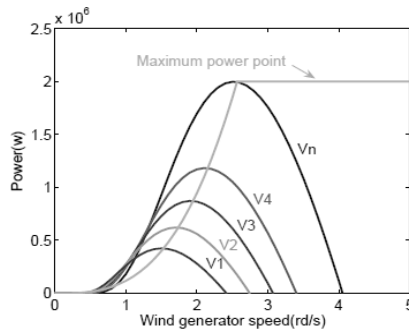


Fig.2. Wind generator power curves at various wind speed.

### B. Modeling of PMSG

Dynamic model of PMSG can be expressed in the synchronous rotating reference frame where the q-axis is 90° ahead of the d-axis. The PMSG modeling is thus given by the armature voltage equations as follows [24]:

$$v_{gq} = R_g i_q + L_q \frac{di_q}{dt} + \omega_e L_d i_d + \omega_e \Psi_f \quad (7)$$

$$v_{gd} = R_g i_d + L_d \frac{di_d}{dt} - \omega_e L_q i_q \quad (8)$$

Where  $L_q$  and  $L_d$  are the inductance of the generator on the q-and d-axis respectively,  $R_g$  is the stator resistance,  $\Psi_m$  is the permanent magnetic flux and  $\omega_e$  is the PMSG electric angular speed.

$$\omega_e = P_n \omega_m \quad (9)$$

$P_n$  is the number of the PMSG pole pairs and  $\omega_m$  is the rotor mechanical angular speed. Where  $i_d=0$ , the expression for the generator electromagnetic torque will be [25]:

$$T_e = \frac{3}{2} p_n \varphi_f i_q \quad (10)$$

Considering the definition of friction coefficient  $F$  and constant of inertia  $J$ , the speed dynamic equation (Newton's law) will be as follows:

$$J \dot{\omega}_m = T_e - T_m - F \omega_m \quad (11)$$

## III. CONTROL SYSTEM DESIGN

### A. MPPT control strategy

The MPPT controller is used to generate the reference speed to activate the wind turbine to extract maximum power from the available wind power [22].

$$\omega_{opt} = \frac{v \lambda_{opt}}{R} \quad (12)$$

The maximum mechanical output of the turbine is given by (13):

$$P_{turbine-max} = \frac{1}{2} \rho A C_{pmax} \left( \frac{R \omega_{opt}}{\lambda_{opt}} \right)^3 \quad (13)$$

Which varies in the different wind speeds. Our task would be, for any available  $V$  (wind speed), to obtain relevant  $\omega_{opt}$  so that by having it,  $P=P_{turbine-max}$ .

### B. Pitch angle control

The pitch angle controller should be able to maintain the wind generator production power at its rated value. There for at the higher wind speeds, in order to prevent the power exceeding from the generator rated level, it will appropriately change the pitch angle. It is needed to acquire the maximum mechanical power of wind speed. At the same time, above maximum rated speed.  $\beta$  should thus be selected such that both conditions are fulfilled. This is shown in the following block diagram:

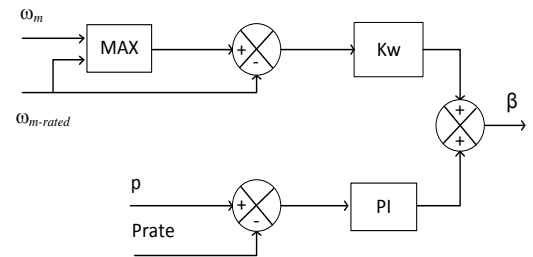


Fig.3. WECS Pitch angle controller.

## IV. CONTROL OF THE GENERATOR SIDE CONVERTER WITH MPPT AND SLIDING MODE CONTROLLER

The MPPT controller used in this paper generates  $\omega_{m-opt}$ , ie , optimized reference speed for application in the generator side converter control system , speed control loop and generation of maximum power by the wind generator.

The generator side three phase converter has been used as a rectifier and the generator performance control at rotor optimized speed  $\omega_{m-opt}$  to capture maximum energy from the wind. In order to control this converter, the sliding mode control strategy has been used [26].

It is inferred from (15) and (11) that the wind turbine speed can be controlled by regulating the stator q-axis current,  $i_{qr}$ . In order to fulfill the sliding mode conditions, the sliding



surface for the wind controller will thus be defined as follows [27]:

$$S_{\omega} = \omega_{m-opt} - \omega_m \quad (14)$$

Depending on wind speed,  $\omega_{m-opt}$  is obtained in the MPPT method from (12). Lyapunov's function, which is positive definite, is defined as [28].

$$\Gamma_{\omega} = \frac{1}{2} S_{\omega}^2 \quad (15)$$

The system stability should be proved using Lyapunov stability theory so that the process of loading the rotor speed to the reference speed  $\omega_{m-opt}$  can be guaranteed. It can be easily established that [29, 30]:

$$\dot{\Gamma}_{\omega} = S_{\omega} \dot{S}_{\omega} < 0 \quad (16)$$

$$S_{\omega} = \dot{S}_{\omega} = 0 \quad (17)$$

Besides, when the sliding mode occurs on the sliding surface:

In order to fulfill this relation, i.e. achieving the sliding surface zero and optimal dynamic performance, the  $U_c$  selected for the system should have generally two parts: a control to hold the system on the sliding surface ( $U_n$ ) and the other one for the system to appropriately behave on the sliding surface ( $U_{eq}$ ) [29].

$$U_c = U_{eq} + U_n \quad (18)$$

$U_{eq}$  can be given from expression  $\dot{S}_{\omega} = 0$ . Thus when the system reaches the sliding surface will not exit from it. For  $U_n$  [30]:

$$u_n = k_{\omega} \text{sgn}(S_{\omega}) \quad (19)$$

where  $k_{\omega} > 0$  and :

$$\text{sgn}(S_{\omega}) = \begin{cases} 1 & S_{\omega} > \varepsilon \\ \frac{S_{\omega}}{\varepsilon} & |S_{\omega}| \leq \varepsilon \\ -1 & S_{\omega} < -\varepsilon \end{cases}$$

where  $\varepsilon$  is a positive constant and should not be taken too low or too high, to guarantee the system dynamic quality will decrease. In order to reduce the generator copper loss  $i_d$  is selected equal to zero. Then, in order to insure the increase of  $\omega_m$  to  $\omega_{m-opt}$ , the appropriate control is effected by determining a reference fit for  $i_q$ .

$$i_{dr} = 0 \quad (20)$$

$$i_{qr} = \frac{2}{3p_n \psi_f} (T_m + J \omega_{m-opt} + F \omega_m + k_{\omega} \text{sgn}(S_{\omega})) \quad (21)$$

with the following choices it is shown that  $\Gamma_{\omega}$  will be negative.

$$\dot{\Gamma}_{\omega} = S_{\omega} \dot{S}_{\omega} = -\mu_{\omega} S_{\omega}^2 + \frac{S_{\omega}}{J} (\dot{\omega}_{m-opt} + T_m + F \omega_m - \frac{3p_n \psi_f i_{qr}}{2} + \mu_{\omega} J S_{\omega}) \quad (22)$$

$\dot{\omega}_{m-opt}$  will be replaced using Eq.(15) and  $i_{qr}$  using Newton's equation. They can be obtained as ( $\mu_{\omega}$  is a positive constant number):

$$\dot{\Gamma}_{\omega} = -\mu_{\omega} S_{\omega}^2 < 0 \quad (23)$$

Asymptotic stability will thus be proved. Using Lyapunov direct method, since  $\Gamma_{\omega}$  is clearly positive definite,  $\dot{\Gamma}_{\omega}$  is negative definite and stability at  $S_{\omega}=0$ , asymptotical stability will be global. Thus, when the time tends to infinity,  $S_{\omega}$  will tend to zero. Besides, all trajectories starting off the sliding surface  $S_{\omega}=0$  must reach it in a limited time and should then remain on this surface. Moreover, a sliding mode control is used to regulate the currents based on their references.

#### A. q-axis current controller design:

The q-axis current controller is used to promote the q-axis current,  $i_q$  to the reference value of  $i_{qr}$ . In order to insure the promotion of  $i_q$  to  $i_{qr}$ , a sliding surface will also be defined for it.

$$S_q = i_{qr} - i_q \quad (24)$$

We proceed to have:

$$\dot{S}_q = \dot{i}_{qr} - \dot{i}_q \quad (25)$$

When the sliding mode occurs on the sliding surface, then:

$$S_q = \dot{S}_q = 0 \quad (26)$$

And as before, with  $\Gamma_q = \frac{1}{2} S_q^2$ , we will define it.

$$V_{qr} = V_{eq-q} + V_{n-q} \quad (27)$$

Solving  $\dot{S}_q = 0$  will give:

$$V_{eq-q} = R_s i_q + L_d \omega_e i_d + \omega_e \psi_f + L_q \dot{i}_{qr} \quad (28)$$

And  $V_{n-q}$  is obtained by the switching sliding surface selection:

$$V_{n-q} = k_q \text{sgn}(S_q) \quad (29)$$

$k_q$  is a positive number. It can be easily proved that  $\dot{\Gamma}_q < 0$ .

By differentiating Lyapunov's function, we obtain:

$$\dot{\Gamma}_q = S_q \dot{S}_q \quad (30)$$

By replacement (28) and (29) in (30) results in:

$$\dot{\Gamma}_q = -\mu_q S_q^2 < 0 \quad (31)$$

Where  $\mu_q$  is a positive constant number

#### B. d-axis current controller design

In order to reduce the copper loss, the controller tries to set the d-axis current on reference value of zero. The sliding surface for the current components  $i_d$  will thus be defined as follows:

$$S_d = i_{dr} - i_d \quad (32)$$



$$\dot{S}_d = \dot{i}_{dr} - \dot{i}_d \quad (33)$$

When the sliding mode occurs on the sliding surface, then:

$$\dot{S}_d = S_d = 0 \quad (34)$$

The control includes two terms in order to obtain commutation around the surface and good dynamic performance:

$$V_{dr} = V_{eq-d} + V_{n-d} \quad (35)$$

Each of the components is determined using (8), (32), (33), (34) and (35), the d-axis control voltage, as follows:

$$V_{eq-d} = R_g i_d - L_q \omega_e i_q \quad (36)$$

$$V_{n-d} = k_d \text{sgn}(S_d) \quad (37)$$

where  $k_d$  is a positive number.

Lyapunov's function for the d-axis current can be written as follows:

$$\Gamma_d = \frac{1}{2} S_d^2 \quad (38)$$

For stability achievement on the sliding surface, it will suffice to have:

$$\dot{\Gamma}_d < 0 \quad (39)$$

Differentiating Lyapunov's function (38), results in:

$$\dot{\Gamma}_d = S_d \dot{S}_d \quad (40)$$

Combining (39) and (40), leads to:

$$\dot{\Gamma}_d = -\mu_d S_d^2 < 0 \quad (41)$$

$\mu_d$  is a positive number. Global asymptotic stability will thus be obtained. Accordingly, the PWM method for control signal generation to implement the nonlinear control for the generator. The doubly closed loop control diagram has been shown in Fig. 4 for the generator side converter.

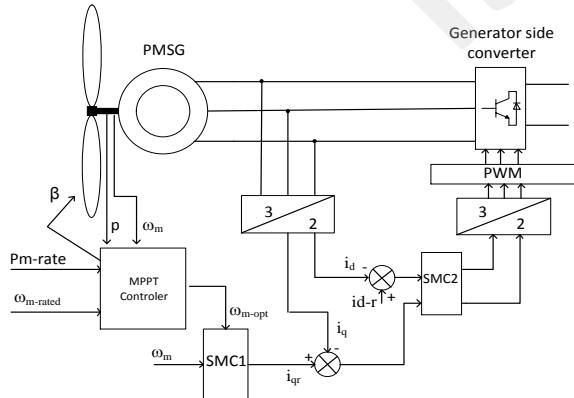


Fig.4.Block diagram of machine side converter controller.

### B. grid side converter controller design

In the  $\alpha\beta$  stationary frame for the circuit linking the grid side converter to the grid (Fig.5), the following equations can be derived:

$$U_{\alpha\beta} = R_f I_{\alpha\beta} + L_f \frac{dI_{\alpha\beta}}{dt} + V_{\alpha\beta} \quad (42)$$

$$P = -1.5[U_{\alpha} I_{\alpha} + U_{\beta} I_{\beta}] \quad (43)$$

$$Q = -1.5[U_{\beta} I_{\alpha} - U_{\alpha} I_{\beta}] \quad (44)$$

By differentiating these two expressions:

$$\frac{dP}{dt} = -1.5[U_{\alpha} \frac{dI_{\alpha}}{dt} + I_{\alpha} \frac{dU_{\alpha}}{dt} + U_{\beta} \frac{dI_{\beta}}{dt} + I_{\beta} \frac{dU_{\beta}}{dt}] \quad (45)$$

$$\frac{dQ}{dt} = -1.5[U_{\beta} \frac{dI_{\alpha}}{dt} + I_{\alpha} \frac{dU_{\beta}}{dt} - U_{\alpha} \frac{dI_{\beta}}{dt} - I_{\beta} \frac{dU_{\alpha}}{dt}] \quad (46)$$

Evidently:

$$U_{\alpha} = U \sin(\omega_1 t) \quad (47)$$

$$U_{\beta} = -U \cos(\omega_1 t) \quad (48)$$

$$\frac{dU_{\alpha}}{dt} = \omega_1 U \cos(\omega_1 t) = -\omega_1 U_{\beta} \quad (49)$$

$$\frac{dU_{\beta}}{dt} = \omega_1 U \sin(\omega_1 t) = \omega_1 U_{\alpha} \quad (50)$$

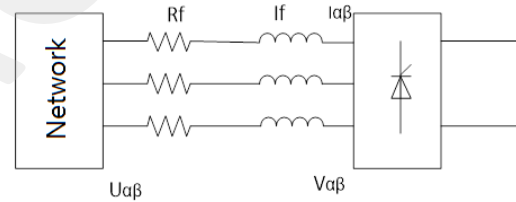


Fig.5.Block diagram of grid side filter.

Combining (42) to (50) results in:

$$\frac{dP}{dt} = -\frac{1.5}{L_f} [U_{\alpha}^2 + U_{\beta}^2 - (U_{\alpha} V_{\alpha} + U_{\beta} V_{\beta})] - \frac{R_f}{L_f} P - \omega_1 Q \quad (51)$$

$$\frac{dQ}{dt} = \frac{1.5}{L_f} [U_{\beta} V_{\alpha} - U_{\alpha} V_{\beta}] - \frac{R_f}{L_f} Q + \omega_1 P \quad (52)$$

The control system aims to promote P and Q to their reference values. The reference value of Q is set to zero to consider the set of the generator and converters from the view point of the grid with unity power factor. The reference value of P is set at a value by which the DC link capacitor voltage has been established and which should not be lower than  $U_{dcref}$ . The sliding surfaces can be initially defined:

$$S_p = e_p = P_{ref} - P \quad (53)$$

$$S_Q = e_Q = Q_{ref} - Q \quad (54)$$

$$\dot{S}_p = \dot{P}_{ref} - \dot{P} \quad (55)$$

$$\dot{S}_Q = \dot{Q}_{ref} - \dot{Q} \quad (56)$$





$$\frac{d}{dt} \begin{bmatrix} S_p \\ S_q \end{bmatrix} = \begin{bmatrix} \dot{P}_{ref} + \frac{1.5}{L_f} [U_\alpha^2 + U_\beta^2] + \frac{R_f}{L_f} P + \omega_1 Q \\ \frac{R_f}{L_f} Q - \omega_1 P \\ \frac{1.5}{L_f} \begin{bmatrix} U_\alpha & U_\beta \\ U_\beta & -U_\alpha \end{bmatrix} \begin{bmatrix} V_\alpha \\ V_\beta \end{bmatrix} \end{bmatrix} \quad (57)$$

$$\dot{S} = F + D.V \quad (58)$$

Lyapunov's function is recommended as follows:

$$W = \frac{1}{2} S^T S \quad (59)$$

$$V = -D^{-1} \left\{ F + \begin{bmatrix} K_{p1} & \text{sgn}(S_p) \\ K_{q2} & \text{sgn}(S_q) \end{bmatrix} \right\} \quad (60)$$

Recommended control:

$$\dot{W} = \frac{1}{2} (S^T \dot{S} + \dot{S}^T S) \\ = S^T \dot{S} = - \begin{bmatrix} K_{p1} & S_p & \text{sgn}(S_p) \\ K_{p2} & S_q & \text{sgn}(S_q) \end{bmatrix} < 0 \quad (61)$$

In order to generate desired  $\dot{P}_{ref}$ , the block diagram in Fig.(6), which is a simple PI controller is used.

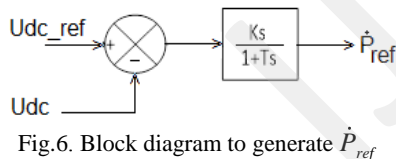


Fig.6. Block diagram to generate  $\dot{P}_{ref}$

## V. SIMULATIONS AND RESULTS

The techniques described above were implemented for the system shown in Fig.4. In MATLAB/Simulink the system is modeled as in Fig. 7.

The system constants and parameters are expressed in the attachment. The speed controller aims at wind maximum energy extraction at powers lower than the rated one, whereas the grid side converter aims at energy transfer from the PMSG side to the utility grid by the DC link voltage regulation and achieving unity power factor.

### A. Speed control

In order to show the effectiveness the proposed controllers in responding to wind speed variations, shown in Fig.7 is considered.

Fig.7. a shows wind speed which varies once 5 seconds and after reaching the previous dynamic repose. Variations are, relative to the base speed of 11 m/s, towards both decrease

and increase, and it is observed in Fig. 7.b that wind speed variations have been well compensated with the turbine control appropriate reaction and rotor angular speed has been established.

### B. Power factor control

Fig. 7.c shows the system power factor from the network point of view for different wind speeds. Evidently, here we expect to observe a power factor much close to the unity. This expectation has been fortunately fulfilled in practice, and it is observed that despite variations at the input power, power factor has been as usual established at a value very much close to unity.

### C. DC link voltage control

Fig.7.d shows the effect of wind speed variations on the DC link voltage. The reference signal generated for the active power injected to the grid and the reference signal appropriate tracking by the PI controller had been so that they have been able to control the DC link capacitor voltage at an optimum level.

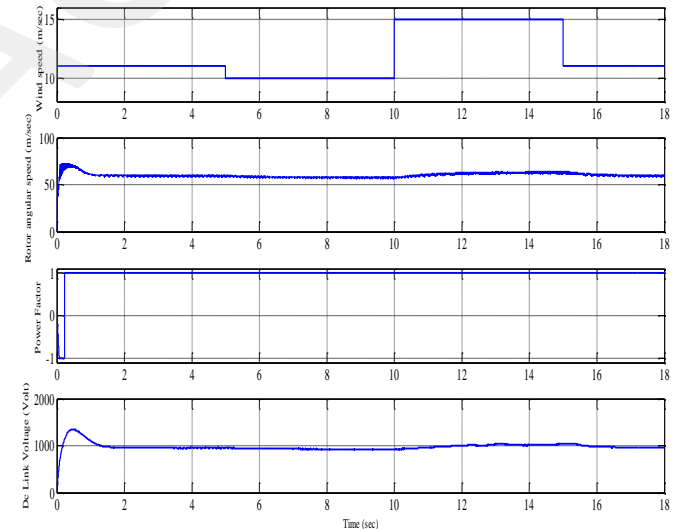


Fig.7. Simulation results. (a) Wind speed (v). (b) Rotor angular speed ( $\omega_m$ ). (c) Power Factor (PF). (d) DC Link Voltage ( $V_c$ )

## VI. CONCLUSION

In this paper, MPPT nonlinear control in the variable speed wind generator based on PMSG has been investigated to increase power transfer to the grid at unity power factor. The system in question includes a wind turbine generator, a PMSG, a PWM rectifier on the generator side and a PWM converter on the grid side connected to each other by the capacitor DC Link. Since the wind generator is nonlinear in nature and has uncertain coefficients and some distortion, the combination of the MPPT strategy technique and the sliding mode nonlinear control method presents an

**International Journal of Digital Application & Contemporary research**  
Website: [www.ijdacr.com](http://www.ijdacr.com) (Volume 2, Issue 7, February 2014)

appropriately acceptable performance. For the pitch angle control regarding wind speed variability, the sliding mode has also been used.

APPENDIX

Table1: System Parameters

Rated Power ( $P_g$ )	8500(W)
Rated Voltage(V)	690(V)
Rated Frequency(F)	50(HZ)
Pole Pairs ( $P_n$ )	5
Rated DC Link Voltage ( $V_c$ )	900(V)
Generator Resistance ( $R_g$ )	0.425( $\Omega$ )
Stator d-Axis Inductance ( $L_d$ )	0.0082(H)
Stator q-Axis Inductance ( $L_q$ )	0.0082(H)
Capacitor Link DC (C)	0.005( $\mu$ F)
Generator Inertial (J)	0.01197(Kg.m <sup>2</sup> )
Friction Coefficient (B)	0.001189(N.m.s)
Rotor Radium (R)	39(m)
Rated Wind speed (v)	11(m/sec)
Area Swept by Blades(A)	4775.94(m <sup>2</sup> )
The Air density ( $\rho$ )	1.225(kg/m <sup>3</sup> )

REFERENCES

- [1] M. O. M. Eknath Vital, Andrew kean, "Rotor Anger Stability with High Penetration of Wind Generation", IEEE TARANSACION ON POWER SYSTEM. Vol 27, pp.353-362. 2012.
- [2] R. K. Rasool Aghatehrani. "Reactive Power Manegment of a DFIG Wind System in Microgrid Based on Voltage Sensivity Analysis", IEEE TRANSACTION ON SUSTAINABLE ENERGY, vol. 2, pp. 451-458. 2011.
- [3] I. E. Stephan Engelhardt, Christan Felter, J. Org. Kretschman, Fekuda Shewarega. "Reactive Power Capability of Wind Turbine Based on Doulby Fed Induction Generator", IEEE TRANSACYION ON ENERGE CONVERSION. 2011.
- [4] T. L. Lasantha Gunaruwan Meegahapola, Damin Flynn. "Decoupled-DFIG Fault Ride-Through Strategy for Enhance Stability Performance During Grid Fault", IEEE TRANSACTION ON SUSTANABLE ENERGY. Vol.27,2010
- [5] C. V. D. S Victor Mendes, Sel enio Rocha Silva, Baldunio Cezar Rabelo, Wilfried Hofman. "Modeling and rid-through control doubly fed induction generator s during symmetrical voltage sags", IEEE TRANSACTION ON ENERGY CONVERSION, vol. 26, 2011.
- [6] S. M. I. Mansor Mohseni, M. A. S Masoum. "Impact of symmetrical and acymmetrical voltage sags on DGIG-Based wind turbine considering phase-angel jump,voltage recovery, and sags parameters", IEEE TRANSACTON ON POWER ELECTRONICS, 2011.
- [7] A. E. M. Azzouz, H. Emara. "Evaluation of fuzzy based maximum power point tracking in wind energy conversion system", IET Renewable power generation. Vol 5, pp. 422-430, 2011.
- [8] M. C. Marcello Pucci. "Neoral MPPT control wind generation with induction machines without speed sensor", IEEE TRANSACTON ON INDUSTRIAL ELECTRONIC. Vol. 58, 2011.
- [9] C. M. H. Whei-Min Lin, Fu Sheng Cheng, "Desing of intelligent controller for wind generation system with sensorless maximum wind energy control", Energy Conversion and Manegment, 2011.
- [10] N. K. M Kesraoui, A. Belkadi. "Maximum power point tracker of wind energy conversion system.Renewable Energy", Vol 36. Pp. 2655-2662, 2011.
- [11] K. H. A. Yunaye Xia, Barry Williams. "Anew maximum power point tracking technique for permanent magnet synchronous generator based wind energy conversion system", IEEE TRANSACTION ON POWER ELECTRONIC. Vol 26. pp. 3609-3620, 2011.
- [12] A. C. C. L. Battasso, Y. Nam, C. E. R. Riboldi. "Power curve tracking in the percent of a tip speed constraint, Renewable Energy, vol. 40,pp. 1-12, 2012.
- [13] L. Y. C. Li Wing. "Redution of power fluctuation of large scale grid connected offshore wind farm using variable frequency transformer", IEEE TRANSACTION ON SUSTANBLE ENERGY. Vol. 2. Pp. 226-234, 2011.
- [14] N. H. M. A. Chawdhury, W.X. Shen. "Smoothing wind power fluctuation by fuzzy logic pitch angel controller", Renewable energy. Vol 38. pp. 224-233, 2012.
- [15] A. P. Akei Uehara, Tomonori Goya, T. Senjyu, Atsushi Yona, N. Urasaki, T. Funnabashi. "A coordinated control method to smooth wind power fluctuation of a PMSG-Based WECS", IEEE TRANSACTION ON ENERGY CONVERSION. Vol 26. Pp. 550-558, 2011.
- [16] A. M. Ronan Doherty, G. Nolan. D. J. Burke. A. Bryson, M. Omalley. "AN assumment of the impact of wind generation system ferequency control", IEEE TRANSACTION ON POWER SYSTEM. Vol. 25. Pp. 452-460, 2010.
- [17] X. yingcheng and T. Nengling. "Reviwe of contribution to frequency control through variable speed wind turbine", Renewable Energy. Vol. 36. pp. 1671-1677, 2011.
- [18] A. B. Jacob Aho, Jason laks. P.feleming. Y. Jeong. F. Dunne, M. Churchfield. L. Pao. K. Jonson. "A Tutarial of wind turbine control for supporting grid frequency through active power control", 2010.
- [19] P. L. Ping-Kwan Keung. H. Banakar, B. T. Ooi. "Kinetic Energey of wind turbine generator for system frequency support", IEEE TRANSACTION ON POWER ELECTRONIC SYSTEM. Vol. 24. Pp. 279-287, 2009.
- [20] F. M. H. O. Anaya- lara, N. Jenkins, G. Strbac. "Contribution of DFIG based wind farm to power system short-term frequency regulation", IEE, Generation, Transmition and Distribution. Vol.153. pp. 164-170, 2006.
- [21] A. M. Juan Manuel Mauricio, A. Gomez-Exposito. J. L. M. Ramos. "Ferequency regulation contribution through variable speed wind energy convection system", IEEE TRANSACTION ON POWER SYSTEM. Vol. 24. Pp. 173-180, 2009.
- [22] S. M. Muyeen, Rion Takahashi, Toshiaki Murata and Junji Tamura, "A Variable Speed Wind Turbine Control Strategyto Meet Wind Farm Grid Code Requirements", IEEE Transactions on power systems, Vol. 25, No. 1, pp. 331 – 340, February 2010,.
- [23] M.A .Abdullah, A.H.M. Yatim, Chee Wei Tan, "A study of maximum power point tracking algorithms for wind energy system", Proceedings of Clean Energy and Technology (CET), IEEE First Conference on, pp. 321 326, 2011.
- [24] Kelvin Tan, and Syed Islam, "Optimum Control Strategies in Energy Conversion of PMSG Wind Turbine System without Mechanical Sensors", IEEE Transactions On Energy, Vol. 19, No. 2, pp 392 - 399, June 2004.
- [25] Y. Errami, M. Ouassaid and M. Maaroufi, "Modelling and Control Strategy of PMSG Based Variable Speed Wind Energy Conversion System", Proceedings of IEEEICMCS' 11, pp.1-6, 2011.
- [26] Zhe Chen, Josep M. Guerrero and Frede Blaabjerg, "A Review of the State of the Art of Power Electronics for Wind Turbines", IEEE

**International Journal of Digital Application & Contemporary research**  
**Website: [www.ijdacr.com](http://www.ijdacr.com) (Volume 2, Issue 7, February 2014)**

- Transactions on power electronics, Vol. 24, No. 8, pp. 1859 - 1875, August 2009.
- [27] Cheng-Kai Lin, Tian-Hua Liu and Li-Chen Fu, " Adaptive Backstepping PI Sliding-Mode Control for Interior Permanent Magnet Synchronous Motor Drive Systems ", Proceedings of American Control Conference on ACC-IEEE, pp. 4075 - 4080, June - July , 2011.
- [28] Utkin V. I, "Sliding mode control design principles and applications to electrical drives", IEEE Trans. on Industrial Electronics, vol. 40, No. 1, February 1993.
- [29] Shaojing Wen and Fengxiang Wang," Sensorless Direct Torque Control of High Speed PMSM Based on Variable Structure Sliding Mode", Proceedings of Electrical Machines and Systems, ICEMS-IEEE, International Conference on , pp. 995 – 998, 2008.
- [30] Djilali Kairous and René Wamkeue , "Sliding- Mode Control Approach for direct power control of WECS based DFIG", Proceedings of Environment and Electrical Engineering IEEEIC-IEEE, 10th International Conference on, pp. 1 – 4, Mai 2011.